Anal. Chem. **2002,** *74,* 4472−4479

Spatial Two-Photon Fluorescence Cross-Correlation Spectroscopy for Controlling Molecular Transport in Microfluidic Structures

Petra S. Dittrich and Petra Schwille*

Experimental Biophysics Group, Max-Planck-Institute for Biophysical Chemistry, Am Fassberg 11, D-37077 Göttingen, Germany

The increasing availability of microfluidic systems of various geometries and materials for the downscaling of chemical or biochemical processes raises a strong demand for adequate techniques to precisely determine flow parameters and to control fluid and particle manipulation. Of all readout parameters, fluorescence analysis of the fluid or suspended particles is particularly attractive, as it can be employed without mechanical interference and with a sensitivity high enough to detect single molecules in aqueous environments. In this study, we present the determination of flow parameters, such as velocity and direction, in microstructured channels by fluorescence correlation spectroscopy (FCS), a method based on single molecule spectroscopy carried out in confocal optical setups. Different modes of FCS, such as auto- and dual-beam cross-correlation techniques by one- and two-photon excitation, are discussed. Known advantages of two-photon excitation, such as highly restricted detection volumes and low scattering background, are shown to be particularly valuable for measurements in tiny channel systems. Although conventional autocorrelation is sufficient for describing the velocity of single molecules, dual-beam cross-correlation allows the separation of isotropic and anisotropic dynamics, for example, to monitor flow directions or to discriminate against photophysical effects that could be mistaken for mobility parameters. It can be shown that time-gated two-photon excitation in the dual-beam mode significantly lowers the undesired cross-talk between the two measurement volumes. Finally, some applications, such as the calibration of microfluidic sorting units and flow profiling, are demonstrated.

"Microfluidics" refers to the design, manufacturing, and practical use of microscale devices that handle very small volumes of fluids on the order of nano- to picoliters. The availability of chip-based channels or capillaries combined with miniaturized pumps, mixers, and valves opens up fascinating prospects to develop versatile total-analysis systems integrated on microscopic geometries (μTAS).[1−3] In recent years, a multitude of possible applications for microfluidic devices has been proposed and introduced. A particularly promising field is the downscaling of various chemical and biochemical processes, including the investigation of reaction kinetics, sensing, and separation of reaction products,[4,5] as well as manipulation and sorting of cells and particles.[6,7] As one of the presently most important topics for biochemical analytics, the detection, sizing, and sequencing of DNA fragments in flowing streams[8−10] should be mentioned.

A crucial requirement for the study of miniaturized systems of any kind is the availability of extremely sensitive control units and readout parameters. In many cases, the measurements are based on fluorescence spectroscopy, allowing fast, sensitive, and selective detection of minute quantities down to the level of single molecules.[11,12] In general, the miniaturization of chemical reaction systems yields a multitude of advantages over macroscale systems; sample consumption as well as reaction times can be strongly decreased because of improved heat exchange due to the high surface-to-volume ratio. Additionally, reactions can be easily parallelized on the microchips. Probably the most important prospects and biggest challenges for future applications lie in the integration of different reaction and manipulation units on a single microstructure where processes can be carried out in an automated routine (so-called lab-on-a-chip). However, the transfer from macro- to microscale is not achieved by the mere downsizing of established setups and geometries. Capillary forces as well as adsorption of sample molecules to the channel walls get signifi-

* Corresponding author. Tel: +49-551-201-1165. Fax: +49-551-201-1435. E-mail: pschwil@gwdg.de.

(1) Mitchell, P. *Nat. Biotechnol.* **2001**, *19*, 717−721.
(2) Stone, H. A.; Kim, S. *AIChE J.* **2001**, *47*, 1250−1254.
(3) McDonald, J. C.; Duffy, D. C.; Anderson, J. R.; Chiu, D. T.; Wu, H.; Schueller, O. J. A.; Whitesides, G. M. *Electrophoresis* **2000**, *21*, 27−40.
(4) Kopp, M. U.; de Mello, A. J.; Manz, A. *Science* **1998**, *280*, 1046−1048.
(5) Gao, J.; Xu, J.; Locascio, L. E.; Lee, C. S. *Anal. Chem.* **2001**, *73*, 2648−2655.
(6) Fu, A. Y.; Spence, C.; Scherer, A.; Arnold, F. H.; Quake, S. R. *Nat. Biotechnol.* **1999**, *17*, 1109−1111.
(7) Furlong, E. E. M.; Profitt, D.; Scott, M. P. *Nat. Biotechnol.* **2001**, *19*, 153−156.
(8) Chou, H. P.; Spence, C.; Scherer, A.; Quake, S. *Proc. Natl. Acad. Sci. U.S.A.* **1999**, *96*, 11−13.
(9) Dörre, K.; Brakmann, S.; Brinkmeier, M.; Han, K. T.; Riebeseel, K.; Schwille, P.; Stephan, J.; Wetzel, T.; Lapczyna, M.; Stuke, M.; Bader, R.; Hinz, M.; Seliger, H.; Holm, J.; Eigen, M.; Rigler, R. *Bioimaging* **1997**, *5*, 139−152.
(10) Van Orden, A.; Cai, H.; Goodwin, P. M.; Keller, R. A. *Anal. Chem.* **1999**, *71*, 2108−2116.
(11) Van Orden, A.; Machara, N. P.; Goodwin, P. M.; Keller, R. A. *Anal. Chem.* **1998**, *70*, 1444−1451.
(12) Zander, C.; Drexhage, K. H.; Han, K. T.; Wolfrum, J.; Sauer, M. *Chem. Phys. Lett.* **1998**, *286*, 457−465.

10.1021/ac025625p CCC: $22.00
Published on Web 07/27/2002

cant, and Rayleigh numbers decrease, which makes it easier to meet certain requirements, such as sustaining laminar flow, but on the other hand complicates mixing and particle exchange. Substantial difficulties arise for channel systems beneath the micrometer scale, like clogging of dirt, settled air bubbles, or leakages at the interface for fluid introduction, which change the fluidic behavior and strongly obstruct the local control of flow parameters. Experimental uncertainty with respect to contamination and other disturbances that can well be below the optical resolution limit renders it crucial to provide a method that enables an easy, fast, and reliable determination of flow properties. Efforts have been made to monitor the fluidic behavior by imaging of highly fluorescent solutions and particles; flow velocity has also been determined by optical Doppler tomography[13] or by fluorescence bleaching techniques in which dye-containing fluids are bleached at a defined spot and detected at another position downstream.[14]

The present paper discusses the precise determination and control of flow parameters by different modes of fluorescence correlation spectroscopy (FCS), a single molecule based technique that selectively analyzes fluctuations in the fluorescence signal, generally induced by dyes or dye-labeled molecules entering and leaving an open detection volume, and by intermittent fluorescence emission during their dwell time in it.[15] In its confocal representation, the detection volume is defined axially by the tight focusing of excitation laser light and laterally by a field diaphragm (pinhole) in the image plane positioned in front of the detector. FCS enables the determination of multiple parameters on a single-molecule scale,[16] in particular, concentrations and mobility coefficients, as well as time constants of internal fluctuations, for example, due to photophysical transitions[17] or reversible intramolecular and intermolecular association/dissociation reactions.[18−20] Moreover, fluctuation analysis by FCS provides the framework to distinguish random diffusion from directed transport,[21] for example, to analyze the flow of fluorescent molecules through the laser focus in microstructured channels[22,23] or along molecular pathways and networks in the living cell.[24]

Although standard FCS does, in fact, allow a very precise determination of flow velocities that are significantly faster than the diffusion time, it exhibits a major drawback by being insensitive to the flow direction as a result of the circular shape of the volume element. In principle, particles being transported through the volume on different tracks from one side to the other could not be distinguished in their resulting FCS flow curves. One way to surpass this problem and increase the accuracy of the flow measurements is by employing two measurement volumes instead of one, that is, two focused laser beams spatially separated by a defined distance, and by cross-correlating the respective emission signals. In case of directed flow, every single fluorophore successively passes the two focused beams, which are preferably aligned in the direction of the flow, resulting in a cross-correlation curve with a distinct maximum that corresponds to the transition time between the volumes. A crucial experimental requirement for the dual-beam setup is a very tight spatial filtering of the two detection volume elements in order to produce minimal overlap and thus, cross-talk, which otherwise results in substantial pseudo-autocorrelation contributions to the measured curves.[25]

Confocal FCS experiments already exhibit high spatial resolution and excellent signal-to-noise ratios. However, it has recently been demonstrated[26] that two-photon excitation, that is, quasi-simultaneous absorption of two low energy (IR) photons, with its tight inherent spatial sectioning[27] can under certain circumstances significantly improve the suppression of out-of focus light in FCS applications. It can be demonstrated here that two-photon excitation, in addition to its benefits of lower scattering background, allows for a dramatic reduction of undesired fluorescence in the spatial regime between the two foci in dual-beam applications: first, because the effective two-photon volume elements for FCS are generally very small as a result of the nonlinear absorption process with its square dependence on excitation intensity; and second, because the pulsed excitation with 80 MHz repetition rate allows for a delayed excitation between the two foci by ∼6 ns, which makes it particularly unlikely for molecules in the interfocal space to be sufficiently excited.

In the following, the theory of flow determination by fluorescence correlation spectroscopy in one- and dual-beam experiments is briefly outlined. In the Experimental Section, the benefits of time-gated two-photon dual-beam cross-correlation (TPE-cc) will be demonstrated by comparing this technique with conventional one-focus autocorrelation, carried out with excitation modes (OPE-ac and TPE-ac) as well as dual-beam cross-correlation for one-photon excitation (OPE-cc). The developed techniques will be applied to precise flow profiling and calibration of fluidic systems in custom-made microstructures designed for the sorting of cells and particles. Finally, the property of dual-beam cross-correlation to eliminate uncertainties in velocity determination produced by photophysical reactions of sample molecules traversing the focused beam will be demonstrated.

THEORETICAL FRAMEWORK

FCS is generally concerned with the temporal analysis of fluctuations $\delta F(t)$ of the fluorescence signal $F(t)$, emitted from dye molecules diffusing through a tightly focused laser beam. In standard autocorrelation applications, the fluorescence intensity fluctuation $\delta F(t) = F(t) - \bar{F}$ with temporal average $\bar{F}$ is compared to the signal at the same position $\vec{r}$ but at a delayed time $t + \tau$. By using two volume elements instead of one, spatial cross-correlation can be facilitated, which relates signal fluctuations at two distinct

(13) Chen, Z.; Milner, T. E.; Dave, D.; Nelson, J. S. *Opt. Lett.* **1997**, *22*, 64−66.
(14) Schrum, K. F.; Lancaster, J. M.; Johnston, S. E.; Gilman, S. D. *Anal. Chem.* **2000**, *72*, 4317−4321.
(15) Elson, E. L.; Magde, D. *Biopolymers* **1974**, *13*, 1−27.
(16) Mets, Ü.; Rigler, R. *J. Fluoresc.* **1994**, *4*, 259−264.
(17) Widengren, J.; Mets, Ü.; Rigler, R. *J. Phys. Chem.* **1995**, *99*, 13368−13379.
(18) Haupts, U.; Maiti, S.; Schwille, P.; Webb, W. W. *Proc. Natl. Acac. Sci. U.S.A.* **1998**, *95*, 13573−13578.
(19) Schwille P.; Kummer S.; Heikal A. A.; Moerner W. E.; Webb W. W. *Proc. Natl. Acad. Sci. U.S.A.* **2000**, *97*, 151−156.
(20) Kettling, U.; Koltermann, A.; Schwille, P.; Eigen, M. *Proc. Natl. Acad. Sci. U.S.A.* **1998**, *95*, 1416−1420.
(21) Magde, D.; Webb, W. W.; Elson, E. L. *Biopolymers* **1978**, *17*, 361−376.
(22) Gösch, M.; Blom, H.; Holm, J.; Heino, T.; Rigler, R. *Anal. Chem.* **2000**, *72*, 3260−3265.
(23) Van Orden, A.; Keller, R. A. *Anal. Chem.* **1998**, *70*, 4463−4471.
(24) Köhler, R. H.; Schwille, P.; Webb, W. W.; Hanson, M. J. *Cell Sci.* **2000**, *113*, 3921−3930.
(25) Brinkmeier, M.; Dörre, K.; Stephan, J.; Eigen; M. *Anal. Chem.* **1999**, *71*, 609−616.
(26) Denk, W.; Strickler, J. H.; Webb, W. W. *Science* **1990**, *248*, 73−76.
(27) Schwille, P.; Haupts, U.; Maiti, S.; Webb, W. W. *Biophys. J.* **1999**, *77*, 2251−2265.

spatial positions to each other. In this case, the temporal development of the fluorescence signals F_1 and F_2 from two volume elements V_1 at the position $\vec{r}$ and V_2 at the position $\vec{r}'$ is considered, resulting in the cross-correlation function.

$$G_{CC}(\tau) = \langle \delta F_1(t,\vec{r}) \delta F_2(t+\tau,\vec{r}') \rangle / \bar{F}_1 \bar{F}_2 \quad (1)$$

As has been previously described by Brinkmeier et al.,[25] the following expression for the cross-correlation function can be derived from eq 1.

$$G_{cc}(\tau) = \left[N\left(1+\frac{\tau}{\tau_d}\right)\sqrt{1+\frac{{\omega_0}^2\tau}{{z_0}^2\tau_d}} \right]^{-1} \exp\left[-\frac{R^2}{{\omega_0}^2} \frac{1}{(1+(\tau/\tau_d))} \left(\frac{\tau^2}{{\tau_{f,cc}}^2} + 1 - 2\frac{\tau}{\tau_{f,cc}} \cos\alpha \right) \right] \quad (2)$$

Herein, the detection efficiency of each focused beam is described using a three-dimensional Gaussian distribution, $W_i(\vec{r})$, in which the size in the radial and axial directions is defined by w_0 and z_0, that is, the $1/e^2$ distance of the light intensity from the central point of the detection elements. Both detection volumes, shifted in the xy plane by the distance R, are assumed to be of equal size, whereas the average residence time of the fluorescent molecules inside of each detection volume due to diffusion is $\tau_d = {\omega_0}^2/4D$ (D = diffusion coefficient).

The flow is assumed to be perpendicular to the z direction enclosing the angle α with the connecting vector $\vec{R}$ of the two volume elements. Additionally, it is considered to be uniform inside the confocal detection volume and constant over the measuring time. The flow velocity can be derived from the flow time, τ_f.

$$\tau_{f,cc} = |\vec{R}|/|\vec{V}_{xy}| = R/v \quad (3)$$

In contrast to fluctuation autocorrelation functions, which show a steady decay, the cross-correlation function in eq 2 exhibits a local maximum at

$$\tau_{max} = -\left(\tau_d + \frac{{\tau_{f,cc}}^2}{2\tau_d}\left(\frac{R}{\omega_0}\right)^{-2} \right) + \sqrt{\left(\tau_d + \frac{{\tau_{f,cc}}^2}{2\tau_d}\left(\frac{R}{\omega_0}\right)^{-2} \right)^2 + {\tau_{f,cc}}^2\left(1+\left(\frac{R}{\omega_0}\right)^{-2}\right) + 2\tau_d\tau_{f,cc}\cos\alpha} \quad (4)$$

This value corresponds to the time that a molecule needs to travel the distance between the two centers of the focal spots. If diffusion can be neglected, due to $\tau_f \gg \tau_d$, eq 2 can be simplified as follows:

$$G_{cc}(\tau) = \frac{1}{N}\exp\left[-\frac{R^2}{{\omega_0}^2}\left(\frac{\tau^2}{{\tau_{f,cc}}^2} + 1 - 2\frac{\tau}{\tau_{f,cc}}\cos\alpha \right) \right] \quad (5)$$

In this case, the maximum τ_{max} approaches $\tau_f \cos\alpha$. If $\alpha = 0$, meaning that both detection volumes are aligned to the flow direction, the location of the maximum ($\tau_{max} = \tau_f$), thus, allows a good estimation of the flow velocity for known R, without even fitting the cross-correlation curves.

In the case of only one volume element, the difference vector $\vec{R}$ is 0, and with

$$\tau_{f,ac} = \omega_0/v \quad (6)$$

the standard autocorrelation function for uniform translation with diffusion is obtained.[21]

$$G_{ac}(\tau) = \left[N\left(1+\frac{\tau}{\tau_d}\right)\sqrt{1+\frac{{\omega_0}^2\tau}{{z_0}^2\tau_d}} \right]^{-1} \exp\left[-\left(\frac{\tau}{\tau_{f,ac}}\right)^2 \frac{1}{(1+(\tau/\tau_d))} \right] \quad (7)$$

The simplified expression for quasi-nondiffusion ($\tau_f \gg \tau_d$) is

$$G_{ac}(\tau) = \frac{1}{N}\exp\left[-\frac{\tau^2}{{\tau_{f,ac}}^2} \right] \quad (8)$$

The above correlation functions for diffusion and flow in one- and two-volume geometries were derived assuming one-photon excitation. In the case of two-photon excitation, the square dependence of the fluorescence signal on excitation light intensity has to be considered. This square dependence results in inherent spatial sectioning of the excitation volume,[27] rendering pinholes in the image plane in principle redundant. However, our experiments have shown that spatial emission profiles $W_i(\vec{r})$ to be approximated by a Gaussian function can be more conveniently realized if pinholes are sustained in the detection system,

$$W_i(\vec{r}) = \kappa {I_0}^2 \exp\left(-4\frac{x^2}{{w_0}^2} \right) xp\left(-4\frac{y^2}{{w_0}^2} \right) \exp\left(-4\frac{z^2}{{z_0}^2} \right) \quad (9)$$

with κ, the detection efficiency of the system, including optical filter losses and fluorescence quantum yield; and I_0, the intensity of the focused beam at the central point.

Consequently, for two-photon excitation, the characteristic diffusion time is $\tau_d = {\omega_0}^2/8D$, and the flow times τ_f for auto- and cross-correlation curves are defined as

$$\tau_{f,ac} = \omega_0/2v \quad (10)$$

$$\tau_{f,cc} = R/2v \quad (11)$$

MATERIALS AND METHODS

Experimental Setup. The experimental setup (Figure 1) was similar to the standard FCS setup described elsewhere.[25,28] The standard dye solution used for the flow measurements was tetramethylrhodamine (TMR) in deionized water with a concentration of ~1nM (OPE) and ~15 nM (TPE). For demonstration of the insensitivity of the dual-beam setup to photophysical effects, the fluorescent protein DsRed (~1 nM in 20 mM NH_4HCO_3 buffer, pH9) was chosen (see Table 1).

For one-photon excitation, the excitation light source was an Ar^+ laser (Lexel) operating at the wavelengths $\lambda = 514$ nm for excitation of TMR and DsRed, and 488 nm for Rhodamine Green

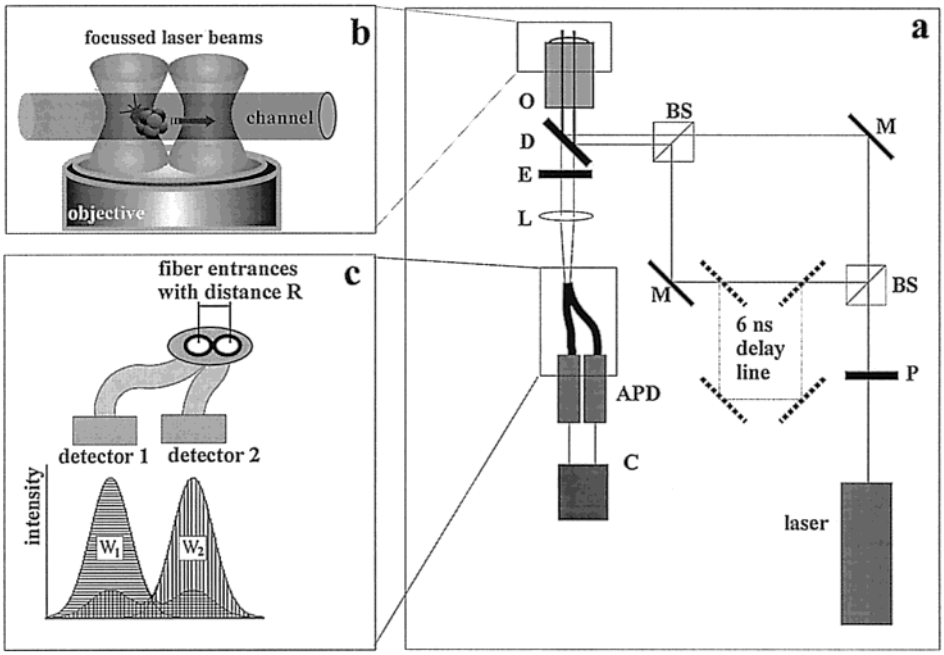

Figure 1. Schematic setup for dual-beam cross-correlation. Part a shows the generation of two parallel laser beams to be coupled into the microscope objective, producing two excitation/detection volume elements in the focal plane. In the case of pulsed two-photon excitation, one beam is delayed by 6 ns to minimize the cross-talk signals (P, $\lambda/2$-plate; BS, beam splitter; M, mirror; O, objective; D, dichroic mirror; E, emission filter; L, lens; APD, detector; C, correlator). The two excitation beams are positioned inside a microfluidic channel (part b) parallel to the flow direction, such that most dye molecules enter both detection volumes successively. The fluorescence signals are projected onto the entrance slits of two bundled optical fibers corresponding to two separate detectors (part c). The effective detection volume of each focused beam, described by $W_i(\vec{r})$, has an additional contribution from not fully suppressed fluorescence being generated in the respective other volume. This cross-talk gives rise to the so-called pseudo-autocorrelation function.

Table 1. Overview of the Different Experimental Conditions, Including the Filter Combinations for the Different Setups[a]

excitation mode (λ_{exc}, intensity)	dye (concn)	dichroic mirror/emission filter
OPE (514 nm, 2×10^5 W/cm^2)	TMR, DsRed (1 nM)	565 DCLP/585DF45
TPE (850 nm, 3×10^6 W/cm^2)	TMR (15 nM)	710 DCSPXR/D600/200
two-beam ac OPE (488 nm, 5×10^4 W/cm^2) TPE (920 nm, 7×10^6 W/cm^2)	Rhodamine Green (10 nM)	500/NIR (special prodution)/HQ 530/60; D600/200

[a] All filters purchased from AHF, Tübingen, Germany.

(see below). The two-photon experiments were carried out using a pulsed titanium−sapphire laser (tunable from 800 to 1050 nm; excitation wavelengths used here, 850 or 920 nm; pulse frequency, 80 MHz; pulse duration, ~100 fs). To guarantee the validity of Gaussian profiles $W_i(\vec{r})$, a significant (~60%) underfilling of the objective back aperture by the laser beams had to be employed for one-photon excitation, resulting in focal waists of ~0.7 μm. For two-photon excitation, overfilled back-apertures could be used. The excitation intensities of the laser beams were chosen below the saturation threshold (2×10^5 W/cm^2 (OPE) and 3×10^6 W/cm^2 (TPE)) such that a linear (respectively, quadratic) dependence of fluorescence on intensity could be observed.

To create two parallel excitation beams for the dual-beam experiments, the excitation light was split and reunited slightly displaced by two polarizing beam splitters. To equalize the intensity of both laser beams, a rotatable $\lambda/2$ plate (adapted either to visible or to IR light) was inserted in the beam path. Both parallel beams were then coupled into an inverted microscope (Olympus IX 70), reflected by a dichroic mirror, and focused by a water immersion objective (Olympus 60× (IR); NA, 1.2) into a microstructured channel, positioned by a *xyz* stage providing additional angular positioning. The fluorescence light was collected by the same objective, and after passing an interference filter for efficient suppression of Raman scattering light (Table 1), it was finally focused onto the apertures of two bundled optical fibers with a diameter of 100 μm and a center distance of ~120 μm. The fluorescence detected through each of the fibers was fed into a separate detector. The photon count signals were correlated quasi on-line by a PC-card ALV-5000 (ALV, Langen, Germany) with typical measurement times of 10 × 10 s. The auto- and cross-correlation curves were fit to the respective models provided above with the PC program Microcal Origin using a Levenberg−Marquardt algorithm. The one-beam experiments were realized simply by blocking one of the split laser beams.

Additionally, a combined one/two-photon two-beam autocorrelation experiment with a solution of 10 nM Rhodamine Green in deionized water was carried out to compare the detection profiles under exactly the same flow conditions. Here, the 488-nm light of the Ar^+ laser with an intensity of 5×10^4 W/cm^2 was combined with the 920-nm light of the pulsed Ti:Sa laser (7×10^6

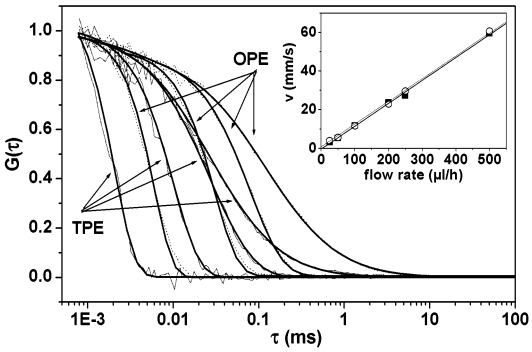

Figure 2. Autocorrelation flow curves (dotted lines) of Rhodamine Green after one- and two-photon excitation with fit curves (solid lines) at different flow velocities given by the flow rate of the syringe pump. Because of the restricted excitation area (the radii of the beam waists are 0.36 μm (for OPE) and 0.25 μm (for TPE)) resulting in a shorter residence time τ_f of the dye in the detection volume, the curves for TPE are shifted to shorter τ. For determination of the velocities (eqs 6 and 10), both excitation modes give identical accuracy (inset).

W/cm^2) by a dichroic mirror (555DCLP, AHF, Tübingen, Germany) and directed into the microscope. For the measurements, either the 488-nm line or the IR-line can be blocked. Since the flow velocity is constant on the spatial and temporal scale used here, this setup enables the direct comparison of flow measurements with one- and two-photon excitation.

Microstructures. The poly(methyl methacrylate) (PMMA) microstructures with integrated channel systems used in the experiments described here were fabricated by Mildendo GmbH, Jena, Germany. The microchips were covered by a 250-μm-thick PMMA cover foil. The channels were 60 μm wide and 40 μm deep, with a steep slope profile. The structure could be precisely positioned by a swivelling *xyz* stage. The positioning could be monitored using the microscope oculars or a CCD camera. The focused beam was usually placed in the middle of a single channel or at the center of the intersection of two channels. The fluid was introduced without further treatment of the channels by a homemade valve and tubing system; the flow velocity could be controlled by changing the height of the water reservoirs or, for fast velocities, by a syringe pump (SP200iw, WPI Inc., Sarasota, FL).

RESULTS AND DISCUSSION

Autocorrelation Flow Analysis with a Single Focal Volume: OPE/TPE. Depending on the flow velocity, the autocorrelation curves were shifted to shorter residence times and typically showed steeper slopes than diffusion curves. This reflects the more uniform distribution of residence times due to the directed transport of the molecule through the focused beam. Figure 2 shows a selection of autocorrelation curves measured at different velocities, *v*, by one- and two-photon excitation in a setup where the detection could be alternated directly between both excitation modes, as described above. For high velocities above ~30 mm/s ($\tau_d \ll \tau_f$), eq 8 describes the measured curves very well. In the case that the directed transport through the focus takes place on the same time range as passive diffusion, eq 7 needs to be used for proper curve fitting. Exact velocity determination by autocorrelation analysis requires a careful calibration of the measurement volume (eqs 6, 10), particularly for the diameter of the beam waist. This is routinely done by measuring an autocorrelation curve of a Rhodamine Green solution, in which only diffusion is present (eq 7 with $\tau_{f,ac} = \infty$).

The influence of the beam waist and the shape of the detection volume on the measured τ_f is demonstrated in an illustrative way by comparing the autocorrelation curves of one- and two-photon excitation measurements for the same flow velocities. It has been reported that two-photon FCS volumes tend to be significantly smaller than standard one-photon volumes because of the inherent spatial filtering of the two-photon process,[26,27] but a remaining uncertainty whether the observed effect of reduced FCS diffusion times was partly due to dynamic photobleaching of the dye molecules could so far not be fully ruled out. Flow measurements with variable velocities, *v*, thus allow a much more reliable comparison, since the influence of bleaching would be less probable at high velocities. It can easily be verified in Figure 2 that the difference between one- and two-photon correlation decay times is preserved for all velocities, *v*. This nicely demonstrates that the differences in residence times indeed reflect the (lateral) dimensions of the two alternative volume elements. The diameter of the two-photon volume (0.5 μm) is a factor of 1.44 $\pm$ 0.1 smaller than the one-photon volume (0.72 μm) in the setup described. A good linear dependence of τ_f on the flow rates regulated by the syringe pump can be verified (see inset) for both one- and two-photon autocorrelation analysis. The inset also shows that the flow velocities calculated from one- and two-photon ac-curves are in excellent agreement, indicating that both excitation modes are suitable for determination of flow velocities faster than a few millimeters per second; i.e., the flow time τ_f is clearly shorter than the characteristic diffusion time τ_d.

Flow Analysis by Dual-Beam Cross-Correlation. Each cross-correlation measurement recorded by the correlator board generates two curves, corresponding to the cross-correlation of signal 1 from the first with signal 2 from the second volume in flow direction (so-called forward correlation $G^{1,2}(\tau)$) and vice versa (backward correlation $G^{2,1}(\tau)$). The subtraction of the backward from the forward curve reveals the "pure" directional transport cross-correlation curve. Figure 3a shows an example of such spatial cross-correlation curves recorded from TMR after one-photon excitation together with the fit function derived from eq 2, which reveals the flow time $\tau_f = 59$ μs and, according to eq 3, the flow velocity of 34 mm/s (R, 2 μm).

An inherent problem of spatial dual-beam cross-correlation is the overlap of the two effective detection volumes in the image plane, that is, the contribution of light emanating from the focal volume which does not correspond to the respective detector or from the interfocal space. Every spatial cross-correlation curve thus exhibits some autocorrelation "background", because each volume element is to a certain extent represented in both detector signals (Figure 1c). The better the two volume elements can be spatially separated, the lower this autocorrelation contribution, and the more pronounced the true cross-correlation signal, which is represented by a symmetric distribution around τ_{max}. It can clearly be seen in Figure 3a that the amplitude of the autocorrelation background is, in case of one-photon illumination of the two volume elements, almost half the total amplitude. By subtraction, the true cross correlation can be revealed. Analyzing the particle numbers according to eqs 2 and 7, we conclude that only ~65%

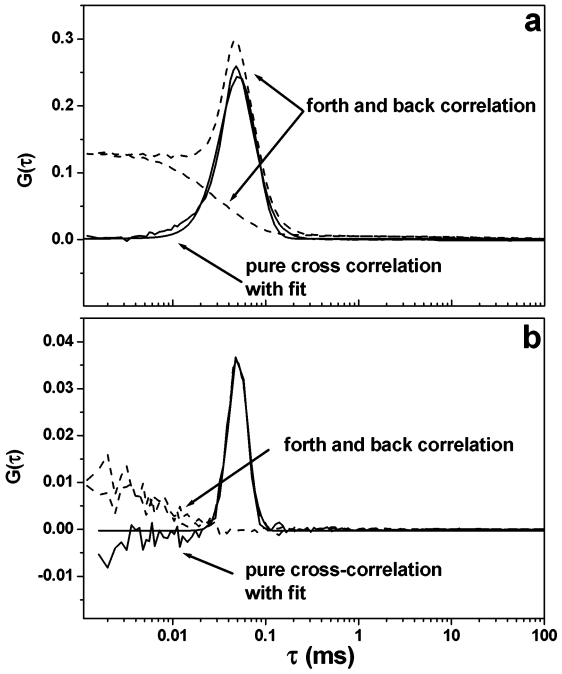

Figure 3. Comparison of back and forth cross-correlation curves of a TMR solution after OPE (a) and TPE (b) for a flow time, τ_f, of ~59 μs. The relationship between the amplitude $G(\tau = 0)$ and the peak height $G(\tau_{max})$ reflects the cross-talk between both detection volumes. The amount of cross-talk, that is, the fraction of molecules detected in both channels, reduces from 35% in part a to 19% in part b. Also shown in either case is the difference curve (pure cross-correlation curve) with the fit (eq 2).

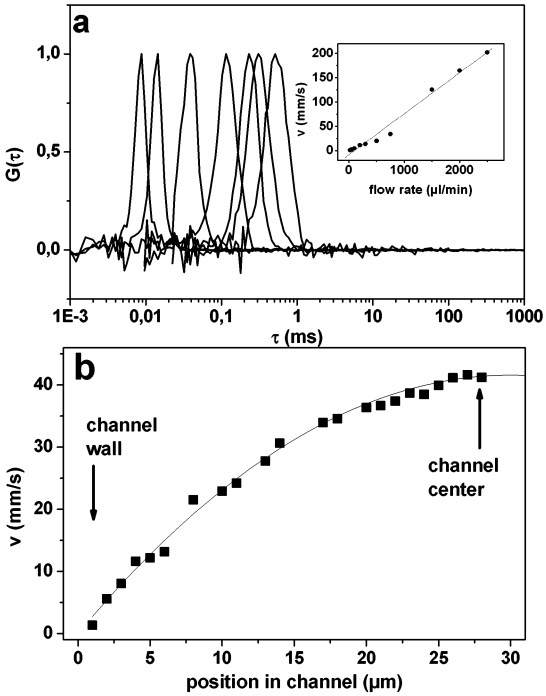

Figure 4. (a) Cross-correlation curves for TMR after two-photon excitation for different flow velocities (0.5−200 mm/s) given by the flow rate of the syringe pump. The inset shows the calibration curve for different flow rates of the syringe pump. (b) Flow velocity in the same channel with a width of 60 μm at different positions. The profile fits with the law of Hagen−Poiseuille for cylindrical channels: $v = \Delta p^*(R^2 - r^2)/4\eta l$ (R, radius; r, position inside the channel during the measurement; η, viscosity of liquid; l, length of channel; Δp, pressure difference).

of all molecules to be detected indeed make the transition from volume 1 to volume 2. The remaining 35% are just to be simultaneously observed by both detectors.

This fraction can be improved to a certain degree by extending the relative distance R/w_0 of the focal volumes. For the mentioned detection fiber system in which the distance between the fiber entrances cannot be changed, this can be accomplished by using an objective with the same NA but lower magnification. However, since the back aperture of the objective is of limited size, the distances of the incoming beams cannot be varied significantly without major distortion of the detection volumes, due to parts of the beams being truncated by entering the objective.

A significant improvement with respect to background autocorrelation can be obtained if two-photon excitation is chosen for illumination. As described above for the autocorrelation measurements, the diameter of the detection volume, w_0, is much smaller after two-photon excitation than after one-photon excitation (see Figure 2), which increases in the case of dual-beam correlation of the relative distance R/w_0 of the two detection volumes. In addition to that, the pulsed excitation with a ~80 MHz pulse repetition rate allows the application of a simple trick to limit the amount of cross-talk fluorescence being generated in the interfocal space. The excitation pulses in both volumes are temporally displaced by 6 ns, which significantly reduces the probability for substantial excitation between the two volumes. Comparative experiments carried out with the same detection pathway thus clearly demonstrate that the autocorrelation cross-talk can be reduced from more than one-third (35%) (Figure 3a) in the case of one-photon excitation to 24% in case of simultaneous two-photon excitation and to less than one-fifth (19%) in the case of time-gated two-photon excitation (Figure 3b). The reduced amplitude $G(0)$ with respect to the peak height $G(\tau_{max})$, as well as the smaller peak width, is clearly perceptible. That means that the two-photon dual-beam cross-correlation methods indeed allow for a more sensitive and precise determination of flow velocities that is particularly important in nonideal geometries, such as cells and narrow microstructures, that generally induce enhanced scattering background signals.

Practical Applications of Dual-Beam FCS. *Determination of Flow Velocity.* Several applications require a precise determination of flow velocity in microstructured channels. For example, in continuous flow modules dedicated to determine reaction kinetics, knowledge about the exact flow velocity is essential to calculate kinetic rate constants. We have demonstrated that flow velocity at a certain position in the channel can be easily determined by FCS analysis. Thus, it is possible to calibrate the velocity of a hydrodynamic flow as a function of the height of the water reservoirs or the speed of the syringe pumps as exemplified in Figure 4a. The characteristic shift of the maximum to the left for increasing flow velocities indicates shorter values of τ_f, from which the flow velocity can be easily derived according to eq 11. The fwhm (full width at half-maximum) values of the curves become smaller at high flow rates as a result of the increased probability that one molecule enters the second volume after having traversed the first. The inset represents the dependence of the flow velocities v on the volume transmission rates of the syringe pump.

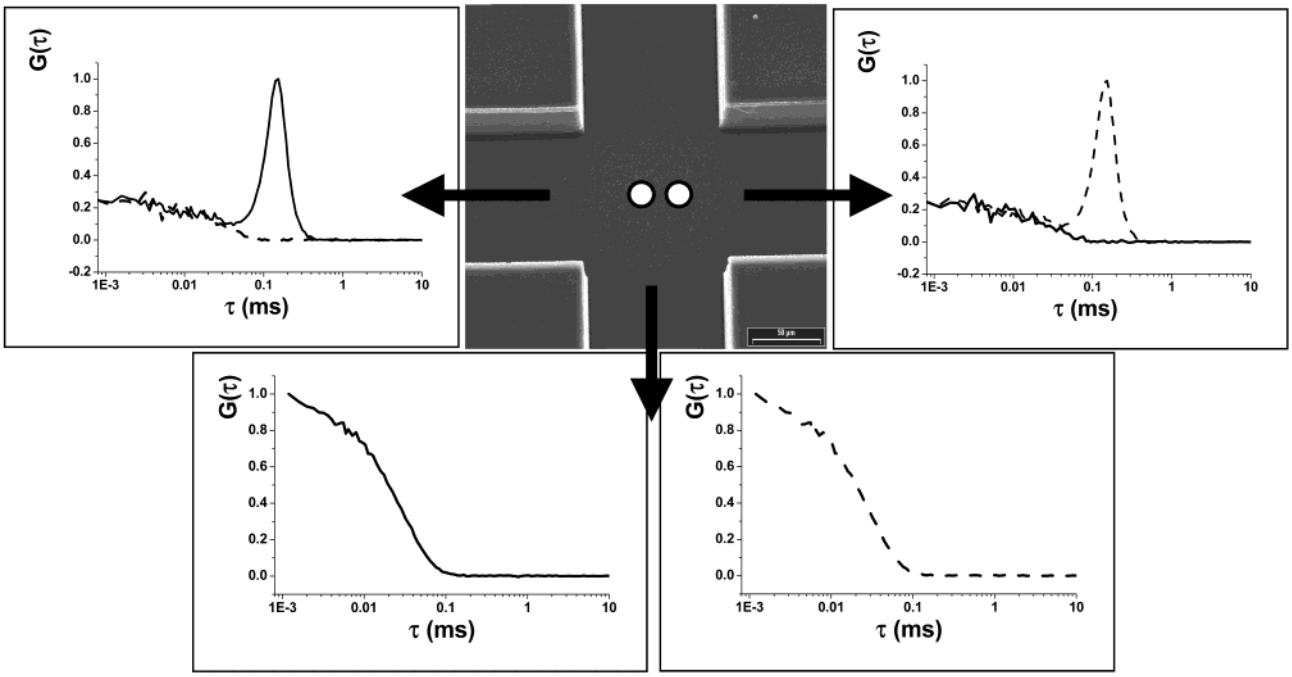

Figure 5. Illustration of the angular dependence of dual-beam cross-correlation. The two focal spots are placed in the cross point of a microchannel system; the arrows designate the flow direction of a TMR solution that gives the shown correlation curves (two-photon excitation; velocity in either direction, 5 mm/s). The change of the flow direction can be evaluated as a result of inverse back and forth correlation. Flow directions perpendicular to the connecting vector of both focused beams result in two equal autocorrelation curves. Less extreme flow changes are demonstrated mainly by changes in the peak height.

It should be mentioned that the range of measurable flow velocity is limited by the time resolution of the detector as well as the correlator board. Since the average flow time, τ_f, depends on the beam waist for the ac measurements and the distance of both foci in the cc (in our setup with $R = 2\ \mu$m, ~3−4 times larger that the beam diameter), higher flow speeds can generally be determined by cc. Additionally, in the dual-beam setup, it is also possible to evaluate transport characteristics that are even slower than the diffusion time inside the volume element.

Because of the highly restricted detection volumes in the one-photon confocal and even more so in the two-photon setup, these calibration measurements can be performed with a very high spatial resolution of fractions of 1 μm in the lateral and axial directions (Figure 4b).

Determination of Flow Direction. As outlined in the theory section, dual-beam cross-correlation provides a valuable means not only to control flow velocity but also to monitor flow directions, as illustrated in Figure 5. In many complex microfluidic structures with T or X junctions designed to combine fluids or to manipulate immersed particles, the control of proper directionality with respect to potential turbulences arising at intersections is of crucial relevance. For example, in the rather extreme case of inverted flow direction, a flip-flop of the forward and backward cross-correlation curves should be observed. If the direction is only remotely changed, the position and height of the maximum of the peak will be changed according to eq 2 (with $\alpha = 0$ and 180, respectively). If the flow direction is perpendicular to the axis connecting the foci, the cross correlation is identical with the autocorrelation cross-talk; i.e., no difference between the backward and forward cross-correlation curves can be found.

Elimination of Photophysical Effects. In contrast to the autocorrelation measurements, internal molecular dynamics that take place on time scales close to the diffusion or transport times, such as the light-induced flickering of fluorophores, such as the red fluorescent protein DsRed[29] or population of the triplet state,[17] do not interfere with the evaluation of the exact flow velocity. Because of the subtraction of the forward and backward cross-correlation curves, where these flow-independent isotropic effects are equally represented, the resulting cross-correlation curve reveals the pure directional transport phenomena. This can be clearly evidenced in Figure 6 showing the normalized auto- (a) and cross- (b) correlation curves of DsRed for different intensities between 10^4 and 3×10^5 W/cm^2 with a flow velocity of approximately 2 mm/s. Because of reversible transitions to a dark state ("flickering") after (one-photon) excitation, the autocorrelation curves exhibit a second characteristic time constant, which could under certain conditions be mistaken for a faster diffusion or transport process. Although different intensities change the shape of the autocorrelation curves, the maximum of the cross-correlation curve stays unchanged; only the peak height $G(\tau_{max})$ varies with the detection signal. Just a slightly increased fwhm at high intensities reflects the distortion (expansion) of both excitation volumes.

CONCLUSIONS

The present study compares different experimental schemes to precisely determine flow and molecular transport properties in microfluidic structures. Whereas the conventional one-focus auto-correlation setup is sufficient for standard velocity measurements in the time range of ~5−200 mm/s, the dual-beam setup

(28) Dittrich, P. S.; Schwille, P. *Appl. Phys. B* **2001**, *73*, 829−837.
(29) Malvezzi-Campeggi, F.; Jahnz, M.; Heinze, K. G.; Dittrich, P.; Schwille, P. *Biophys. J.* **2001**, *81*, 1776−1785.
(30) Sako, Y.; Minoghchi, S.; Yanagida, T. *Nat. Cell Biol.* **2000**, *2*, 168−172.
(31) Heinze, K. G.; Koltermann, A.; Schwille, P. *Proc. Natl. Acad. Sci. U.S.A.* **2000**, *97*, 10377−10382.

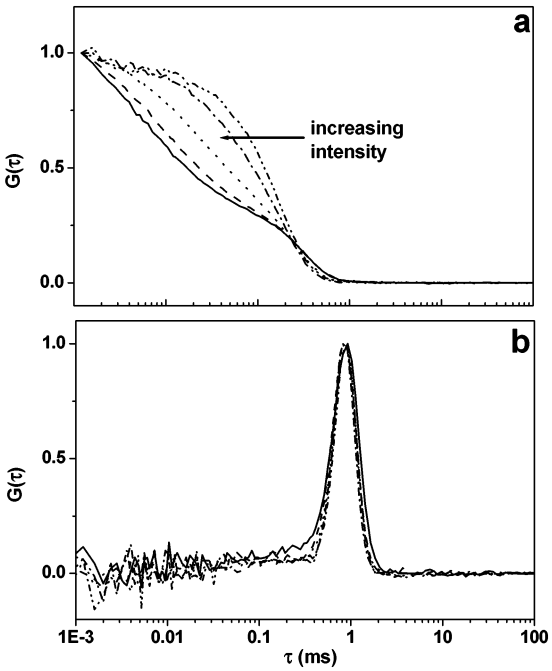

Figure 6. Elimination of internal molecular reactions by dual-beam cross correlation. In this example, DsRed is excited with a 514-nm laser line at different excitation intensities (10^4 to 5×10^5 W/cm^2). Because of the intensity-dependent flickering between a dark and a bright state in a time range of a few microseconds,[29] the auto-correlation curve exhibits a characteristic shape (a), whereas the cross-correlation curves (b) stay unchanged with respect to the place of the maximum ($G(\tau_{max})$).

exhibits several further advantages: The cross-correlation curves, which are unaffected by isotropic effects without spatial coordination, are much less corrupted by photophysical dynamics, reveal even slow directed transport phenomena, and have the extremely valuable capacity to directly monitor changes or alteration of flow direction. Comparing one- and two-photon excitation, it can further be found that the detection volume elements for two-photon excitation can be made substantially smaller by increasing the resolution of the flow measurements. In conjunction with the possibility of time-delayed pulsed excitation in dual-beam setups, it enables a far better suppression of autocorrelating cross-talk, accompanied by a low scattering signal of the infrared light. This particular improvement certainly opens up exciting perspectives for the potential applications of two-volume cross-correlation in living cells, in which many processes with a clear directionality can be observed. Directed transport of molecules to or from certain organelles within the frameworks of protein or membrane trafficking or signal transduction supposedly plays a key role in many processes that are right now about to be studied on a single-molecule level.[30]

In the context of cellular applications, but also for complex reaction systems in microstructures, the demonstrated possibility to combine the two-volume FCS mode with two-photon excitation is of particular importance. The most promising perspective is certainly the dual-color feature that has recently be opened up by two-photon excitation.[31] An extension of the two volume setup to a joint two-volume/two-color setup is easily conceivable, since the IR light can indeed be employed to simultaneously excite spectrally distinct fluorophores.

ACKNOWLEDGMENT

We thank Jure Derganc (U. Ljubljana) for practical advice and Guido Böse and other group members for discussions. Financial support was provided by the German Ministry of Education and Research (Grants Nos. 0311845 and 16SV1257) and Evotec OAI, Hamburg.

Received for review March 13, 2002. Accepted June 25, 2002.

AC025625P